Известия Уральского государственного горного университета. 2020. Вып. 3(59). С. 7-18

Науки о Земле
Earth sciences

УДК 549.514.81+549.02(620)

https://doi.org/10.21440/2307-2091-2020-3-7-18

Morphological and geochemical features of zircon from intrusive rocks of El Sela area, Eastern Desert, Egypt

Mohamed Mahmoud Fathy GHONEIM[1, 2*]
Elena Gennad'evna PANOVA[1**]
Ahmed El Sayed ABDEL GAWAD[2***]
Svetlana Yur'evna YANSON[1****]

[1]Saint Petersburg State University, Saint Petersburg, Russia
[2]Nuclear Materials Authority, Cairo, Egypt

Abstract

The intrusive rocks in El Sela area can be arranged from the oldest to the youngest into: two-mica granite and post-granitic dikes which include microgranite, dolerite and bostonite dikes. Zircon is the most abundant accessory mineral. Zircon morphology and geochemical features are good indicators for evolution of rocks. The aim of the work is to determine the morphology, internal structure and chemical composition of zircon to identify the difference of zircon in various intrusive rocks. Results show that morphologically, zircon in the two-mica granite is euhedral coarse- grained with zonation. It is represented by crystals up to 125 μm and corresponds to S10 and P2. Zircon in post-granitic dikes exhibit irregular forms. Geochemically, zircon crystals have higher ZrO_2 values in the core whereas HfO_2, UO_2, ThO_2 increase at the peripheries of zoned crystals of the two-mica granite. Zircon of two-mica granite contains high HfO_2, UO_2, ThO_2 and CaO contents but low Sc_2O_3 content. HfO_2 is not detected in zircon of microgranite. TiO_2 in zircon of two-mica granite and bostonite dikes is under detection limits. REEs are not recorded in zircon of the studied intrusive rocks.

Keywords: zircon, morphology, geochemical features, intrusive rocks, El Sela, Egypt.

Introduction

The Arabian-Nubian Shield (ANS) is an exposure of Precambrian crystalline rocks on the flanks of the Red Sea. The crystalline rocks are mostly Neoproterozoic in age. Geographically – and from north to south – the ANS includes the nations of Jordan, Egypt, Saudi Arabia, Sudan, Eritrea, Ethiopia, Yemen, and Somalia. The ANS was the site of some of man's earliest geologic efforts, principally by the Egyptians to extract gold from the rocks of Egypt and NE Sudan. The Arabian-Nubian Shield is believed to be the next major exploration frontier in Africa, like West Africa's mineral exploration boom. The ANS mineral potential has yet to be fully explored and extends into the countries Egypt, Sudan, Eritrea, Ethiopia, Djibouti and Saudi Arabia. It hosts a variety of deposits including mesothermal gold, polymetallic quartz vein and volcanogenic massive sulfide ore deposits. Variant ore deposits including zircon, gold, copper, zinc, tantalum and silver are hosted into it. The dominant deposit types are volcanogenic massive sulfide ore deposits and gold quartz vein deposits [1].

Zircon is one of the most important accessory mineral of intrusive rocks, which crystallize in wide scope of P–T conditions. The difference of its crystal morphologies depends on the magma type, aluminum-alkali balance, chemistry of granites and temperature of crystallization [2]; therefore, zircon is considered as tracers of petrogenesis of granites. Generally, it occurs as small early formed crystals often enclosed in later minerals and may form large well-developed crystals (consisting of prism and bipyramids) in granite and pegmatite rocks. The metamict state (breakdown of the structure) in zircon may be due to the presence of radioactive atoms. The metamictization process causes radial and concentric fractures, which represent good pathways for uranium leaching or addition [3, 4].

Many researchers have extensively studied chemistry and typology of zircons from some Egyptian and worldwide granite rocks [5–22].

El Sela is considered as a region of uranium mineralization in Egypt. The aim of this work is to investigate zircon from intrusive rocks and its relation with U–Th elements in its crystal structures and find features of its difference.

Tasks are to determine the morphology, internal structure and chemical composition of zircon to identify the difference of zircon in various intrusive rocks.

✉moh.gho@mail.ru
https://orcid.org/0000-0002-3795-476X
**e.panova@spbu.ru
***ahm.elsay@hotmail.com
****svetlana.janson@spbu.ru

Geologic setting

Numbers of studies were carried out in El Sela shear zone, covering various aspects like: detailed geological, structural, spectrometric survey, geochemical, mineralogical, geophysical methods of uranium exploration [23–37].

El Sela area is characterized by rugged topography with low to high relief and comprises different rock types of the basement complex of the Pre-Cambrian age. Two-mica granite occupies the major part of the studied area which displays the remnants of circular and/or arc-shaped granitic plutons (3 × 5 km) trending ENE–WSW and NNW–SSE parallel to shear zones (Fig. 1). The mentioned granite is usually medium- to coarse-grained and characterized by the hypidiomorphic granitic textures. Granite plutons are divided into several bodies separated by sandy corridors with highest peaks rise to as high as 557 m (above sea level). Two-mica granite is pink to pinkish grey colors. El Sela two-mica granite is mainly composed of quartz, K-feldspar, plagioclase, muscovite and a small amount of biotite.

El Sela two-mica granite is dissected by two perpendicular shear zones. The first shear zone is extending ENE–WSW with about 1.5 km in length and ranges between 5 to 40 m in width. It extends to 6 km in the eastern part of the mapped area with narrow width varies between 3 to 5 m. From the structural point of view, shear zone is dissected by the NW–SE dextral strike-slip faults, NNW–SSE, NNE–SSW and N–S sinstral strike-slip faults (Fig. 1). The ENE-WSW shear zone is characterized by moderate relief. It is highly tectonized, altered and enriched in secondary visible U-mineralization and pyrite megacrysts. This shear zone is invaded by a large number of microgranite, dolerite and bostonite dikes, and quartz and jasper veins.

Microgranite dikes are injected into the two-mica granite along the ENE–WSW shear zone and dipping 72°–83° S. These dikes are fine-grained, ranging in width from 3 to 20 m and extends 6 km SW from the northern margin of El Sela plutons. Microscopically, microgranite consists of plagioclase, to a lesser extent K-feldspar and quartz.

Dolerite dikes have ENE–WSW and NNW–SSE trends. The first trend in which dolerite is parallel to the first shear zone, strikes N–75° and dips 68°–81° S, adjacent and/or

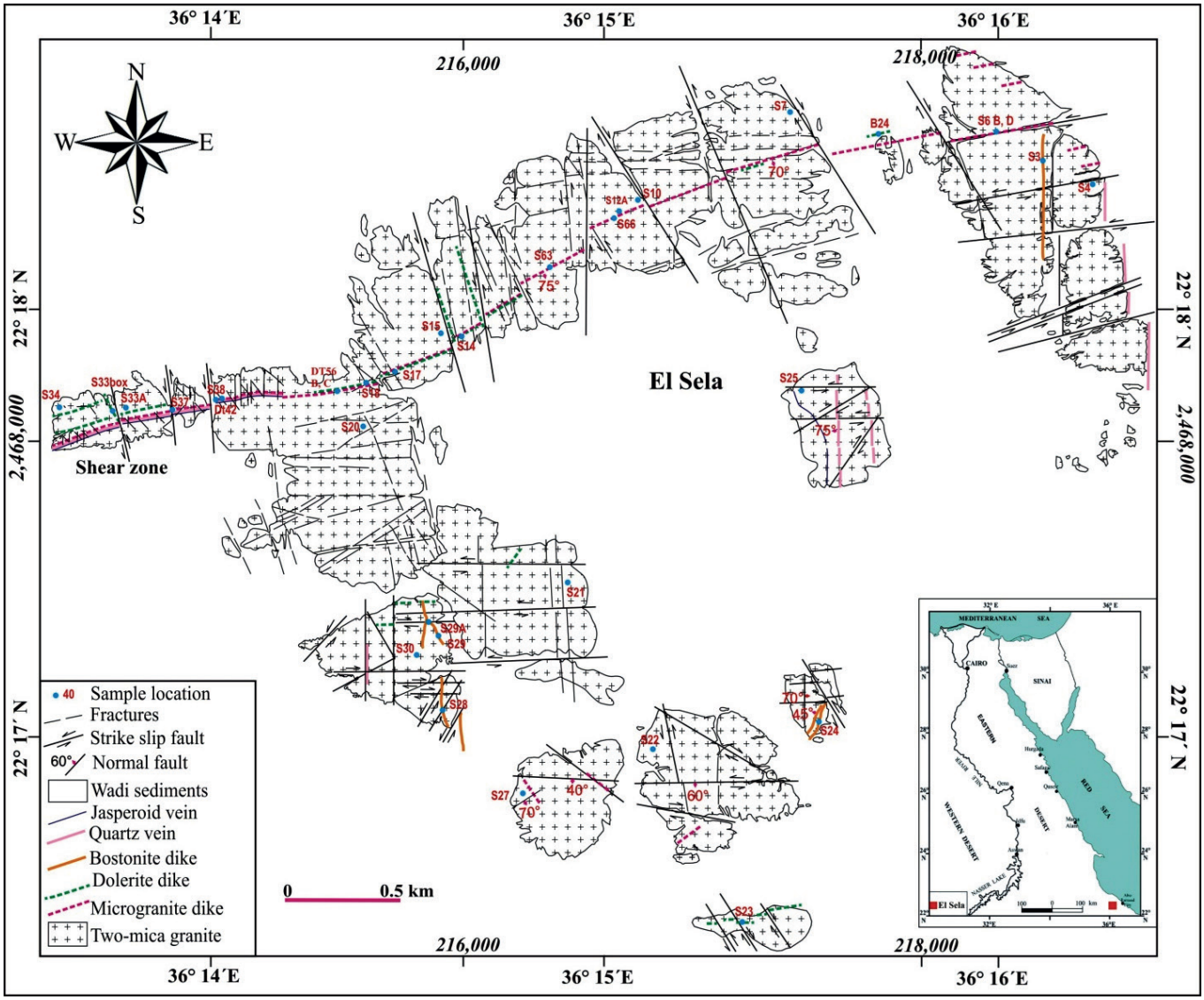

Figure 1. Geologic map of El Sela area, Eastern Desert, Egypt after [23, 25, 28, 33].
Рисунок 1. Геологическая карта района Эль-Села, Восточная пустыня, Египет по [23, 25, 28, 33].

parallel to microgranite dikes in the main shear zone of the mapped area. Microscopically, dolerite dikes are mainly composed of plagioclase, pyroxene, megacrysts of sulphides, iron oxides and visible secondary U-mineralization.

The second shear zone extends NNW–SSE for a short distance (100 m). Dolerite dikes also range in thickness from 1–1.5 m and invade in perpendicular trend the first shear zone and they can act as chemical traps for uranium mineralization.

Bostonite dikes invade granitic plutons along the N–S and NNE–SSW tectonic trends. They are usually fine-grained, reddish brown, sheeted, and range in thickness from 0.5 to 2 meters. The NW-SE strike slip fault (right lateral) cross cut N–S bostonite dike. They are composed of K-feldspar, quartz, pyroxene and iron oxides.

Milky quartz vein dissects the two-mica granite along the ENE-WSW shear zone. This vein is not radioactive, brecciated and ranges in thickness from 1 to 4 m. The milky quartz vein is dissected by red and grey to black jasper veins.

Red and grey to black jasper veins are strongly jointed, fragmented, brecciated and range between 0.5 and 1 m thick, contain visible pyrite megacrysts and uranophane minerals.

Materials and methods

Samples were collected from all types of rocks of El Sela. The analyzed samples are shown on the geologic map which include two-mica granite, microgranite, dolerite and bostonite (Fig. 1). The analyses of Zr were carried out by ELAN-DRC-6100 Inductively Coupled Plasma-Mass Spectrometry (ICP–MS) at the Central Laboratory of All Russian Geological Institute (VSEGEI) after digestion of the fused beads with $HF+HNO_3$. Pure solution external standards were used for calibration, and geological (USGS) standards were used to monitor the analytical accuracy. The precision of ICP-MS for Zr is 0.1 ppm. The results of the chemical analyses of Zr are quoted in (Table 1).

Scientific research were performed at the center for microscope and microanalysis of the research park using Scanning Electron Microscope equipped QUANTA 200 3D (FEI, the Netherlands, 2006), which is mounted on the base of an analytical complex Pegasus 4000 (EDAX, USA). The analyzed zircon data was obtained using Electron Microprobe equipped with CAMECA SX100 using the following conditions: the diameter of the analyzed area on the specimen surface is under 1 μm at standard conditions (15 kV acceleration potential, 15 nA beam current, sample: iron oxide; volume: 3×10^{-19} m^3; mass: 2×10^{-12} g). The microprobe is equipped with 5 automated wavelength-dispersive spectrometers (WDS) and an energy-dispersive spectrometer (EDS), whereas spectrometer range (0.22 to 0.83) sin-theta with a resolution of 10^{-5}. Natural standards albite for Al (Kα), orthoclase for Si (Kα), wollastonite for Ca (Kα), hematite for Fe (Kα), olivine for Mg (Kα) and monazite for Yb (Lα), whereas the synthetic compounds are UO, ThO_2, ZrO_2, $PbCrO_4$, YPO_4, $CePO_4$, $NdPO_4$, $SmPO_4$, GdTiGe and $DyRu_2Ge_2$ which used as standards for U (Mβ), Th (Mα), Zr (Lα), Pb (Mα), Y (Lα), Ce (Lα), Nd (Lα), Sm (Lα), Gd (Lα) and Dy (Lα), respectively. EPMA analyses of Zr are quoted in (Table 2, 3).

Results and discussion

Morphology and internal structure

Zircon SEM images (back scattered or secondary electrons) can be used to study the morphological features of zircon. The most important characteristics are discussed briefly below:

Morphologically, zircon in two-mica granite is euhedral, coarse-grained with zonation (Fig. 2, a, b, d, e, f) and the other type is fine grained (is attributed to sudden cooling) without zonation whereas, zircon in post-granitic dikes exhibits irregular forms with no zonation.

The irregular forms of some zircon grains might be attributed to their growth concomitant with corrosion and interaction

Table 1. Representative chemical analyses of Zr of intrusive rocks in El Sela, Eastern Desert, Egypt, ppm.
Таблица 1. Типичный химический анализ Zr интрузивных пород Эль-Селы, Восточная пустыня, Египет, г / т.

Rock-type	S. No.	Zr, ppm	Rock-type	S. No.	Zr, ppm
Two-mica granite	S4	85.1	Microgranite	S6D	465
	S6B	82.9		S37	360
	S7	85.1		S38	297
	S10	217		Dt42	101
	S 12A	36.9		DT56B	283
	S15	125		DT56C	131
	S 20	69.3	Dolerite	S 14	317
	S21	117		S 17	445
	S 22	65.4		S 23	234
	S 25	60.8		B24	390
	S 27	68.2		S 33 box	500
	S 30	92	Bostonite	S 3	777
	S 33A	50.7		S 24	900
	S34	114		S 28	598
				S 29	674
				S 29 A	576

with the residual melts. The euhedral zircon forms indicate crystallization under favorable and stable conditions. The great similarities in both morphology and internal structures of most zircon grains indicate crystallization from the same magma. Some studies [38–40] related the crystal shape of zircon to the chemical composition of the magma from which it crystallized.

Many parameters are responsible for zircon fractures, which may include external parameters, such as external pressure, rapid pressure release or external stresses and internal parameters such as expansion due to radiation or metamictization [41].

Zircons can keep their original shape even under most severe conditions of metamorphism. Almost rounded grains are indicative of shearing associated with metamorphism, erosion or resorption, while more angular grains (Fig. 2, d) often reflect the growth of primary crystals that have not experienced disturbances [14].

Overgrowths are represented in considerable amount. Both the parallel and elbow twinning are relatively common in zircon of two-mica granite (Fig. 2, f). The studied zircons have some inclusions which are mainly thorite, zircon, opaques and dust. Thorite inclusions occur as white spots (Fig. 2, c, d, e, f). These inclusions are haphazardly oriented. Some zircon crystals are free of inclusions.

Cracks observed in some zircon grains may have resulted from the action of external forces during or after metamorphism, breakage during thin section preparation, presence of many inclusions. However, the cracks in the outer rim (Fig. 2, e) may have been produced by the difference in the chemical composition between core and rim, particularly U, Th, Y and Hf contents. Alteration starts along cracks and affects specific narrow crystallographic zones. If the net of cracks becomes denser, more alteration occurs. In extreme cases alteration also affects previously unaltered zones changing finally the entire crystal with some remaining unaltered islands. The unaffected grains often show concentric zoning, weak in BSE images (Fig. 2, e).

Zoned zircon of two-mica granite

A texture developed in zircon crystals is characterized optically by changes in the color or extinction angle of the mineral from the core to the rim. Back scattered electron BSE images are used to reveal some information about the morphology and internal structure of the studied intrusive rocks. The zircon in two-mica granite show a distinctive oscillatory zonation for some investigated crystals (Fig. 2, a, b). Oscillatory zoning is a common feature in zircons from acidic igneous rocks and is believed to have formed during long periods of crystallization. This feature supports the hypothesis that the

Table 2. Representative EPMA analyses data of zoned crystals zircon of two-mica granite, El Sela area, Egypt, wt%.
Таблица 2. Типичные микрозондовые анализы зональных кристаллов циркона двуслюдяного гранита, район Эль-Села, Египет, мас.%.

Oxides	Core					Rim		
	Spot analyses							
	4428	4429	4430	4437	4438	4435	4440	4441
SiO_2	33.3	31.42	31.83	31.17	31.1	27.7	30.9	30.0
ZrO_2	65.0	62.5	62.5	62.9	62.8	57.4	61.9	58.2
HfO_2	2.1	2.15	2.35	1.85	1.91	3.48	2.06	2.9
UO_2	Bdl	1.6	1.51	0.88	1.01	4.49	1.99	2.72
ThO_2	Bdl	Bdl	Bdl	Bdl	Bdl	0.65	Bdl	Bdl
Y_2O_3	Bdl	Bdl	Bdl	Bdl	Bdl	1.21	Bdl	Bdl
Fe_2O_3	Bdl	1.27	1.49	Bdl	1.34	2.07	1.89	3.27
CaO	Bdl	0.43	Bdl	1.27	0.88	2.49	0.76	1.78
MnO_2	Bdl	0.59	0.6	1	1.01	0.52	0.73	0.87
Sum	100	99.9	100	99.2	100	100	100	99.8
Chemical formula based on 4 oxygen atoms								
Si	1.02	0.98	0.99	0.97	0.97	0.91	0.96	0.95
Zr	0.97	0.95	0.94	0.96	0.95	0.92	0.94	0.9
Hf	0.02	0.02	0.02	0.02	0.02	0.03	0.02	0.03
U		0.01	0.01	0.01	0.01	0.03	0.01	0.02
Th						0		
Y						0.02		
Fe		0.03	0.03		0.03	0.05	0.04	0.08
Ca		0.01	0	0.04	0.03	0.09	0.03	0.06
Mn		0.01	0.01	0.02	0.02	0.01	0.02	0.02
Sum of cations	2	2.01	2.01	2.02	2.02	2.06	2.02	2.05

Bdl – below detection limit (0.01%).

Table 3. Chemical composition of zircon of different rock types, El Sela area, Eastern Desert, Egypt, (oxides in wt.%).
Таблица 3. Химический состав циркона из различных типов горных пород, область Эль-Села, Восточная пустыня, Египет (оксиды в мас.%).

Oxides	Two-mica granite						Average	Microgranite			Average	Dolerite			Average	Bostonite			Average
SiO_2	32.30	30.80	29.00	31.00	30.10	29.90	30.52	34.90	31.67	31.19	32.59	30.21	30.09	30.90	30.40	31.36	30.84	31.60	31.26
ZrO_2	61.80	61.70	59.87	59.40	60.00	60.48	60.54	62.20	63.55	64.15	63.30	59.20	59.41	60.20	59.60	60.26	61.32	60.95	60.84
HfO_2	1.86	1.53	1.69	2.19	2.00	2.21	1.91	Bdl	Bdl	1.14	0.38	Bdl	Bdl	Bdl	Bdl	0.80	1.50	1.76	1.35
CaO	1.39	2.18	3.89	1.12	1.96	1.61	2.02	0.10	0.77	0.90	0.59	0.63	0.43	0.39	0.49	1.76	0.77	0.30	0.94
Fe_2O_3	0.67	0.94	1.49	0.89	2.00	2.13	1.35	0.50	0.60	0.67	0.59	3.26	1.52	1.84	2.21	1.23	1.40	0.90	1.18
TiO_2	Bdl	Bdl	Bdl	Bdl	Bdl	Bdl	Bdl	Bdl	1.82	Bdl	0.61	Bdl	Bdl	3.07	1.02	Bdl	Bdl	Bdl	Bdl
Al_2O_3	0.09	0.94	1.27	1.13	0.72	0.64	0.80	1.23	0.87	1.25	1.11	2.02	3.50	1.70	2.41	2.44	1.80	1.10	1.78
Y_2O_3	Bdl	0.48	1.57	Bdl	Bdl	Bdl	0.34	Bdl	Bdl	Bdl	Bdl	2.57	2.49	1.14	2.07	1.00	1.19	2.96	1.72
Sc_2O_3	Bdl	Bdl	Bdl	Bdl	Bdl	Bdl	Bdl	0.95	0.10	0.20	0.42	0.67	0.67	0.31	0.55	1.18	1.23	0.40	0.94
ThO_2	0.39	0.57	Bdl	2.99	1.72	1.09	1.13	Bdl	Bdl	Bdl	Bdl	Bdl	Bdl	Bdl	Bdl	Bdl	Bdl	Bdl	Bdl
UO_2	1.46	0.81	1.26	1.29	1.49	1.99	1.38	Bdl	Bdl	Bdl	Bdl	Bdl	Bdl	Bdl	Bdl	Bdl	Bdl	Bdl	Bdl
Sum	99.96	99.95	100.04	100.01	99.99	100.05	99.99	99.88	99.38	99.5	99.59	98.56	98.11	99.55	98.75	100.03	100.05	99.97	100.01
Chemical formula based on 4 oxygen atoms (apfu)																			
Si	1.00	0.96	0.91	0.97	0.95	0.94	0.96	1.10	1.00	0.98	1.02	0.95	0.95	0.97	0.96	0.95	0.95	0.97	0.96
Zr	0.93	0.93	0.92	0.91	0.92	0.93	0.92	0.95	0.97	0.98	0.97	0.91	0.91	0.92	0.91	0.89	0.92	0.92	0.91
Hf	0.02	0.01	0.02	0.02	0.02	0.02	0.02			0.01	0.00					0.01	0.01	0.02	0.01
Ca	0.05	0.07	0.13	0.04	0.07	0.05	0.07	0.00	0.03	0.03	0.02	0.02	0.01	0.01	0.02	0.06	0.03	0.01	0.03
Fe	0.02	0.02	0.04	0.02	0.05	0.05	0.03	0.01	0.01	0.02	0.01	0.08	0.04	0.04	0.05	0.03	0.03	0.02	0.03
Ti									0.04		0.01			0.07	0.02				
Al		0.03	0.05	0.04	0.03	0.02	0.03	0.05	0.03	0.05	0.04	0.07	0.13	0.06	0.09	0.09	0.07	0.04	0.06
Y		0.01	0.03				0.01					0.04	0.04	0.02	0.03	0.02	0.02	0.05	0.03
Sc								0.03	0.00	0.01	0.01	0.02	0.02	0.01	0.02	0.03	0.03	0.01	0.02
Th				0.02	0.01	0.01	0.01												
U	0.01	0.01	0.01	0.01	0.01	0.01	0.01												
Sum of cations	2.03	2.05	2.09	2.03	2.05	2.05	2.05	2.14	2.09	2.07	2.10	2.09	2.10	2.11	2.10	2.07	2.05	2.03	

Bdl – below detection limit (0.01%).

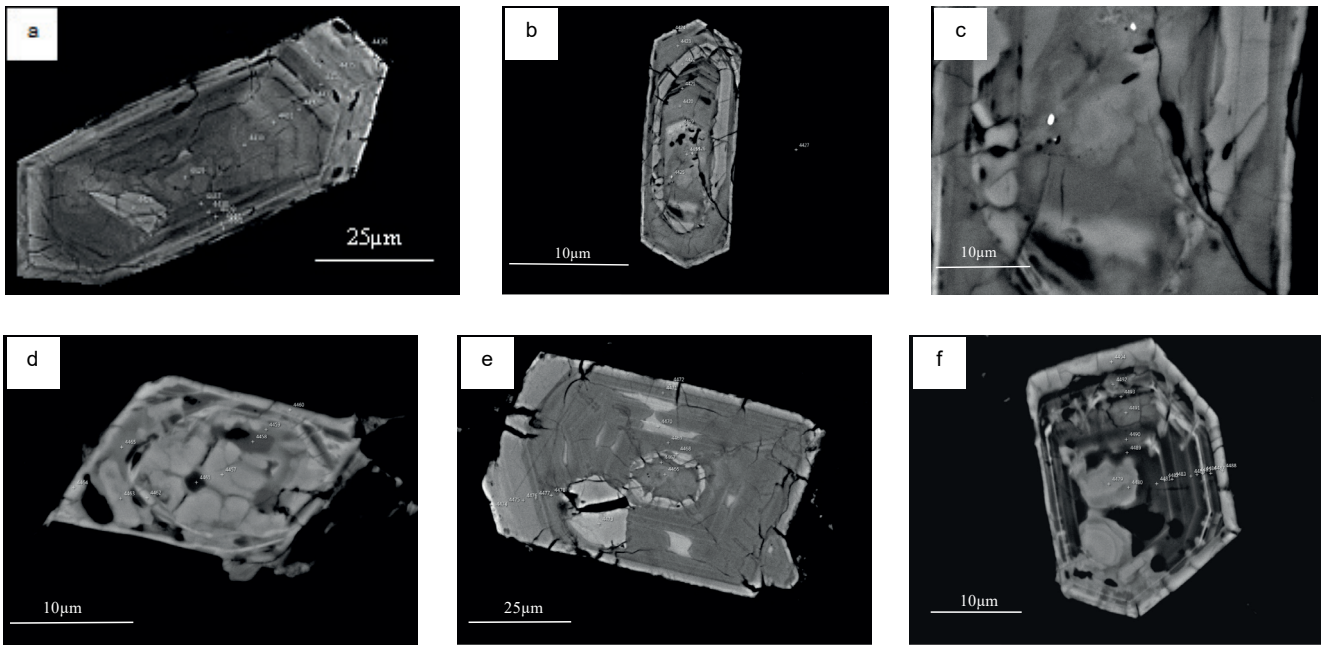

Figure 2. Backscattered electron photomicrographs of zircon crystals in two-mica granite, El Sela, Egypt. a–b – oscillatory zoning; c – inclusions of thorite (white points); d – angular zircon crystal poiclitically enclose opaque with elongated zircon crystal; e – concentric zoning is very weak and cracks in outer rim of zircon crystal; f – zoned zircon with two cores inside

Рисунок 2. Микрофотографии в отраженных электронах кристаллов циркона в двуслюдяном граните, Эль-Села, Египет. a – b - осцилляторная зональность; c – включения торита (белые точки); d – угловатый кристалл циркона обрастающий непрозрачный удлиненный кристалл циркона; e – кристалл циркона со слабой концентрической зональностью и трещинами на кайме; f – зональный циркон с двумя ядрами внутри.

majority of zircons from two-mica granite crystallized in the deep-seated magma chambers, and is further supported by the presence of two zircon nuclei centers present in one grain (Fig. 2, d, e, f).

The zircon nuclei display magmatic oscillatory zonation, and have rounded forms indicating a complex crystallization/resorption process had taken place over a long period of time. It seems likely that such a complex crystal growth history could only be achieved from the zircon residing for long periods of time in different magma batches. The oscillatory zoning of zircons is locally overprinted, probably by changes in fluid composition and perhaps by loss of U, Th, Pb, that accompanied this process [42].

Zircon typology and Pupin diagrams

Natural zircon belongs to the tetragonal crystal system. It usually shows prismatic habit with {100} and {110} prisms and terminated with {101} and {211} pyramids. The probability of combination of the pyramids and prisms faces with variable sizes give chance to arise of several zircon types [43]. Other supplementary pyramid forms may be included give rise to more secondary types and subtypes. The extra {301} pyramid can exist but with a minor development as in the K and V25 subtypes. Based on dimensional crystal statistics, [44] summarized the results of the typo-morphological study of zircon populations in a schematic diagram "zircon habit chart" (Fig. 3), in which each type of morphology is characterized by two coordinates, the prismatic index *T* and the pyramidal index *A*. They observed that the morphology depends on the temperature, chemistry and the available water content. The *A* index (I.A) is positively correlated with the Al/K+Na ratio. The T index (I.T) is directly and positively correlated with the temperature of zircon crystallization. A high *T* index ({100} prim) indicates a higher temperature than does a low *T* index ({110} prism), thus a geothermometric scale was proposed [45]. The {211}, {101} and {301} pyramids are respectively well developed in aluminous, alkaline and hyperalkaline medium. It is observed that the late overgrowths of hydro zircon rich in radioactive elements are prismatic following {110} instead of {100} [46]. This habit change could be related with the action of water.

Zircon typology in El Sela two-mica granite

Suitable crystals have been separated for the zircon typological classification after Pupin (1980). The zircon crystals demonstrate preferential development of {101} pyramid and notably the occurrence of the {211} pyramid with the dominance of the {100} prism. The flat -{101} pyramid of the S and P-types are commonly larger than the steep -{211} pyramid. Zircon originated in a hyperalkaline or hypoaluminous medium have well developed {101} pyramid [38]. Most typically, the two-mica granite of El Sela area shows minor typological distribution forming mainly two distinct morphological types (Fig. 3). It is represented by crystals up to 125 μm and corresponds to P2 (70%) and S10 (30%). Mainly, they are located along the central right hand-side part of the typology diagram with high A-index and moderate *T*-index. The P-type is the major type with relative frequency of 70%. Pupin (1980) suggested that the S and P types show a distinct spreading propensity in potassium-rich alkaline medium. This zircon population is nearly similar to population of I-type alkaline series granite [38].

Geochemical characteristics of zircon

Zircon is one of the mainly distributed accessory minerals in the El Sela area. Zirconium concentrations in two-mica granite vary from 36.9 to 217 ppm with an average of 90.8

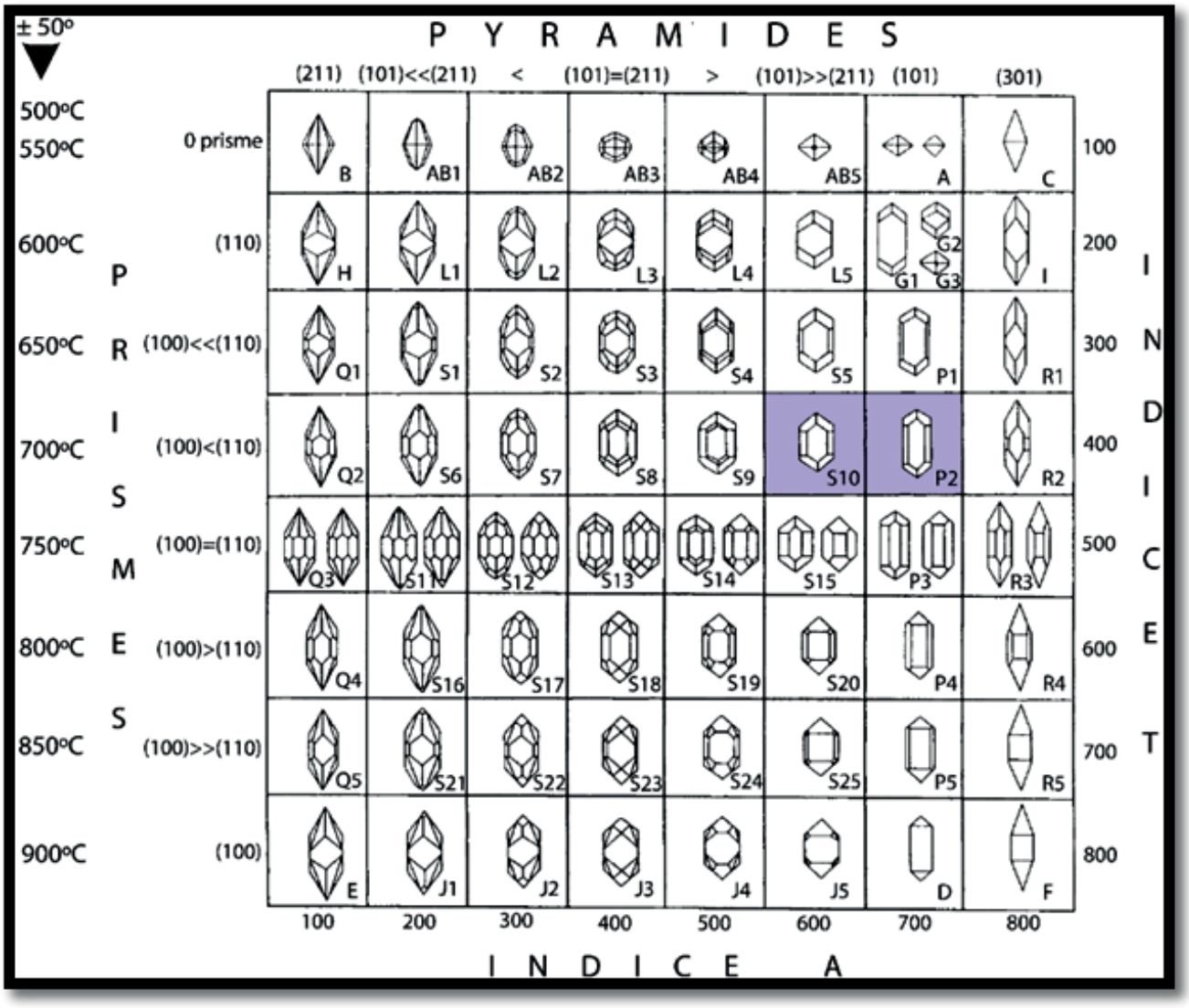

Figure 3. Zircon typological classification proposed by [38]. Index *A* reflects the Al/alkali ratio, controlling the development of pyramids in the crystals. Index *T* reflects the effects of temperature on the development of prisms, zircon of two-mica granite of El Sela area, Eastern Desert, Egypt.

Рисунок 3. Типологическая классификация цирконов, предложенная [38]. Индекс А отражает соотношение Al / щелочь, контролирующее развитие пирамид в кристаллах. Индекс Т отражает влияние температуры на развитие призм, в цирконе двуслюдяного гранита района Эль-Села, Восточная пустыня, Египет.

ppm. Zr contents in microgranite vary from 101 to 465 ppm of Zr with an average of 273 ppm. Zr in dolerite varies from 317 to 500 ppm with an average of 411 ppm, while in bostonite Zr values range from 576 to 900 ppm with an average of 705 ppm (Table 1).

Zircon conforms to the general formula ABO_4, where the position A represents the relatively large zirconium ion in eight-fold coordination with O, and position B represents the silicon ion in tetrahedral coordination with O. In position A, Zr can be replaced by tetravalent (M^{4+} = Hf, Th, U), trivalent (M^{3+} = REE, Y, Fe), and divalent cations (M^{2+} = Ca, Fe, Mg, Mn). As summarized by [14], there are multiple mechanisms of substitution, including simple isovalent replacement of Zr by other tetravalent cations, and coupled substitutions where divalent and trivalent cations may be incorporated.

On the other hand, studies of alteration in zircon show that these elements (especially Ca and Fe, but also Al and Ti) may be secondarily enriched in the altered zones of zircon crystals [47]. For example, [48] studied experimentally the interaction of metamict zircon with hydrothermal fluids, and they observed a gain of solvent cations (e.g., Ca, Ba) from the hydrothermal solution, and the loss of variable amounts of M^{4+} cations (Zr, Si, Hf, Th, U) as well as M^{3+} cations (REE).

The EPMA analyses of zoned zircon of two-mica granite indicate that the core has ZrO_2 ranges (from 62.5 to 65.01 wt%), SiO_2 ranges from (31.1 to 32.42 wt%), HfO_2 ranges from (1.8 to 2.1 wt%), and UO_2 ranges from (0.8 to 1.6 wt%). The rim has ZrO_2 ranges from (50.4 to 57.1 wt. %), SiO_2 ranges from (30 to 31 wt. %), HfO_2 ranges from (2.8 to 4.5 wt. %), UO_2 ranges from (2.9 to 4.4 wt. %), in (Table 2). ZrO_2 has higher values in the core whereas UO_2, ThO_2 and HfO_2 increase at the peripheries of crystals. P_2O_5 is absent so, no xenotime overgrowth is observed. Y_2O_3 may occur only at the crystal rim. Lack of Y_2O_3 with up to 3 wt% was reported by [17] in rare metal granitoids and associated rocks, [27] in El Sela area and [49] in Variscan granites.

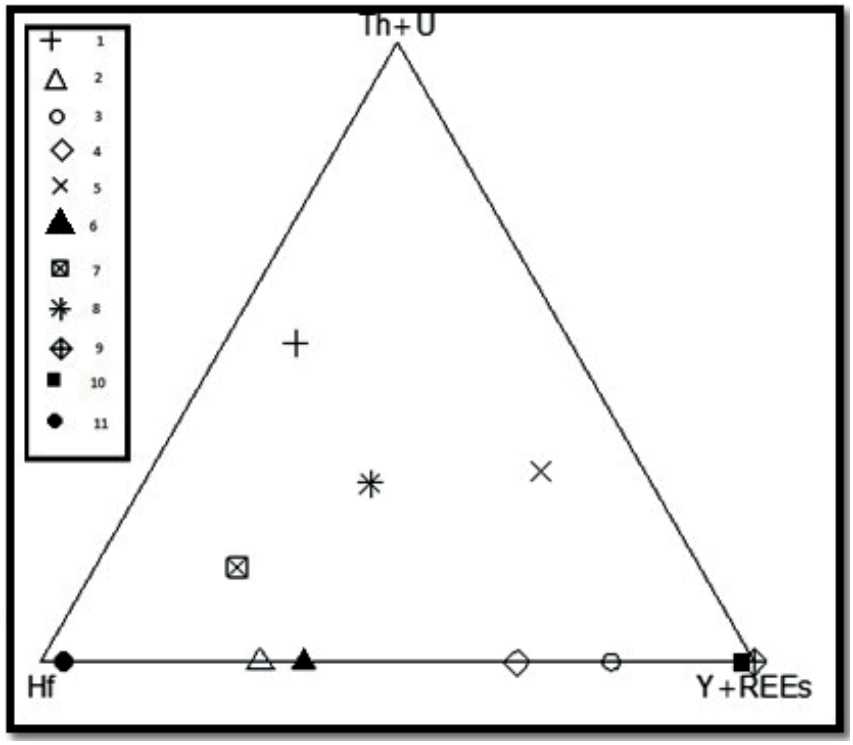

Figure 4. Hf–(U+Th)–(Y+REE) ternary diagram of zircon compositions in intrusive rocks. 1 – Two-mica granite El Sela (present work, 14 samples); 2 – Microgranite El Sela (present work, 6 samples); 3 – Dolerite El Sela (present work, 5 samples); 4 – Bostonite El Sela (present work, 5 samples); 5 – Syenogranite Nikeiba, Egypt (unpublished data, 4 samples); 6 – Granite with black quartz first phase, Salminski massive, Russia, [51] (4 samples); 7 – Two-mica granite, El Sela area, [27] (8 samples); 8 – Two-mica granite, Ghadir, Egypt, [27] (5 samples); 9 – Rare metal granites, Primoria, Russia, [51] (12 samples);10 – Precambrian granites, South Priladaja, Russia, [52] (12 samples); 11 – Rapakivi granites first phase, Salminski massive, Russia, [51] (8 samples).

Рисунок 4. Hf– (U + Th) - (Y + REE) тройная диаграмма состава циркона в интрузивных породах. 1 – Двуслюдяной гранит El Sela (данная работа, 14 образцов); 2 –- микрогранит El Sela (настоящая работа, 6 образцов); 3 – Долерит Эль Села (данная работа, 5 образцов); 4 – бостонит El Sela (данная работа, 5 образцов); 5 – сиеногранит Никиба, Египет (неопубликованные данные, 4 образца); 6 – Гранит с черным кварцем первой фазы, Салминский массив, Россия, [51] (4 образца); 7 – двуслюдяной гранит, район Эль-Села, [27] (8 образцов); 8 – двуслюдяной гранит, Гадир, Египет, [27] (5 образцов); 9 – Редкометалльные граниты, Приморье, Россия, [51] (12 образцов), 10 – Граниты докембрия, Южное Приладожье, Россия, [52] (12 образцов); 11 – Граниты Рапакиви первой фазы, Салминский массив, Россия, [51] (8 образцов).

Table 4. Comparison of chemical composition of (Y+REE), Hf, (Th+U) intrusive rocks of El Sela area with others in Egypt and Russia.
Таблица 4. Сравнение химического состава интрузивных пород (Y + REE), Hf, (Th + U) района Эль-Села с другими в Египте и России.

Zircon samples	Symbol no.	Y+REEs, %	Hf, %	Th+U, %
Two-mica granite El Sela (present work), *n* = 14	1	10,00	38.50	51.50
Microgranite El Sela, (present work), *n* = 6	2	30.70	69.20	0,00
Dolerite El Sela, (present work), *n* = 5	3	80,00	20,00	0,00
Bostonite El Sela, (present work), *n* = 5	4	66.70	33.30	0,00
Syenogranite Nikeiba, Egypt (unpublished data), *n* = 4	5	54.60	14.50	30.80
Granite with black quartz first phase Salminski massive, Russia, [51], *n* = 4	6	36.80	63.10	0,00
Average El Sela two-mica granite, [27], *n* = 8	7	19.80	64.80	15.40
Average of two-mica granite, Ghadir, Egypt, [27], *n* = 5	8	31.70	39.40	28.90
Rare metal granites Primoria, Russia, [51], *n* = 12	9	99.80	0.09	0.02
Precambrian granites South Priladaja, Russia, [52], 2011, *n* = 12	10	99.90	0.03	0.04
Rapakivi granites first phase Salminski massive, [51], *n* = 8	11	3.22	96.70	0,00

Elements were calculated to each other in percentage, %.
Элементы рассчитывались относительно друг друга в процентах, %.

A marked decreasing ZrO_2/HfO_2 ratio from the core to the rim of zircon crystal in the two-mica granite is consistent with a decreasing ZrO_2/HfO_2 ratio of zircons from mafic to felsic rocks. An increasing of UO_2 and ThO_2 content from core to rim of zircon crystal in the two-mica granite which described above is consistent with an increasing trend of the UO_2 and ThO_2 contents from ultra-mafic to felsic rocks as referenced by [50].

Normal zoning of the two-mica granite is displayed by Hf, Y, U and Th in zircon owing to disequilibrium between the interacting fluids and the growing zircon crystals. The disequilibrium state is brought about by sudden change in the pH (alkalinity increased) or temperature (intermitting boiling during pressure release) [17].

The composition of zoned zircon crystals depends on magma type that they crystallized in and ionic properties. Goldschmidt's rule shows that Zr^{4+} has a small radius (0.098 nm) enter zircon crystals relatively earlier than the large ions U^{4+} and Th^{4+} (0.114 and 0.118 nm, respectively). Zr^{4+} enters zircon crystal a little earlier than Hf^{4+}, owing to a small electronegativity 1.21 of Zr^{4+} relatively to 1.38 of Hf^{4+} according to Ringwood's modification to Goldschmidt's rule. This indicates a relatively high Zr^{4+} content in the core than outer rim and also, high content of U^{4+}, Th^{4+} and Hf^{4+} in the rim of a magmatic zircon crystals than inner core. The composition evolution of magmatic rocks and the crystal chemical properties of zircon, such as Zr, Hf, U and Th, are relatively stable. Therefore, the differences in chemical composition zonation trends, especially the HfO_2, (UO_2+ThO_2), and ZrO_2/HfO_2, of zircons are generally fixed, and consequently can be used as the indicators for magmatic zircons [50].

Hf-(U+Th)-(Y+REE) ternary diagram of zircon compositions of intrusive rocks shows that zircon of two-mica granite of the present work, previous work of zircon of two-mica granite of the same area, Egypt [27], zircon from two-mica granite of El Ghadir area, Egypt [27] and zircon from syenogranite of El Nikeiba area, Egypt are located in nearby area in the center, where as zircon from rapakivi granites first phase Salminski massive, Russia [51], zircon from granite with black quartz first phase, Salminski massive [51], Russia, zircon from rare metal granites Primoria, Russia [51], zircon from Precambrian granites south Priladaja, Russia [52], zircon from microgranite, dolerite and bostonite dikes of the present work are located on the Hf, Y and REEs axis with no uranium and thorium contents in (Table 4) and (Fig. 4). REE is not recorded in zircon of intrusive rocks of El Sela area (Tables 2, 3).

The chemical composition of zircon is represented in Table 3. There are some indications can be deduced from zircon microprobe analyses. For instance, zircon from two-mica granites have the highest HfO_2, UO_2, ThO_2 and CaO contents, but the lowest value of Sc_2O_3. There is no detected HfO_2 or Y_2O_3 in zircon from microgranite or dolerite dikes, respectively. TiO_2 in zircon of two-mica granite and bostonite is under detection limits.

Conclusions

Zircon is one of the most abundant accessory mineral of intrusive rocks (two-mica granite, microgranite, dolerite and bostonite dikes) of El Sela area, Egypt. Morphologically, zircon of two-mica granite is euhedral coarse-grained with zonation represented by crystals up to 125 μm and corresponds to S10 and P2 types. It also occurs as fine-grained crystals. Zircon in post-granitic dikes exhibits irregular forms with no zonation.

Geochemically, ZrO_2 has higher values in the core whereas UO_2, ThO_2 and HfO_2 increase at the peripheries of crystals. Y_2O_3 occurs only at the crystal rim. Zircon displays significant covariation in UO_2, ThO_2 and HfO_2. In two-mica granite zircon contains the highest HfO_2, UO_2, ThO_2 and CaO contents, but the lowest value of Sc_2O_3. No detected HfO_2 or Y_2O_3 in zircon of microgranite or dolerite dikes, respectively. TiO_2 in zircon of two-mica granite and bostonite is under detection limits.

Acknowledgments

The authors acknowledge the members of Geomodel Research Center, Saint Petersburg State University, Russia for their assistance in electron microprobe and ICP–MS analyses.

REFERENCES

1. Johnson P. R., Woldehaimanot B. 2003, Development of the Arabian-Nubian Shield: perspectives on accretion and deformation in the northern East African Orogen and the assembly of Gondwana. *Geological Society London Special Publications*, vol. 206, pp. 289–325. http://dx.doi.org/10.1144/GSL.SP.2003.206.01.15
2. Pupin J. P. 1976, Signification des caractères morphologiques du zircon commun des roches en pétrologie: base de la méthode typologique: applications. Thèse de doctorat: Sciences. Université de Nice. Laboratoire de Pétrologie-Minéralogie, Nice, France, 394 p.
3. Read H. H. 1984, Rutley's elements of mineralogy. Delhi, India: Published by S. K. Jam for CBS Publishers and Distributors, 560 p.
4. Deer W. A., Howie R. A., Zussman J. 1992, An introduction to the rock-forming minerals. 2nd edition. London: Longman Scientific & Technical, 696 p. https://doi.org/10.1180/minmag.1992.056.385.20
5. Khaffagy M. B. 1964, The granites of Aswan and their accessory zircons. Unpublished M. Sc. thesis, Assuit University, 192 p.
6. Hussein H. A., Faris M. I., Makram W. 1965, Radioactivity of some accessory minerals especially zircon in some Egyptian granites and pegmatites. *J. Geol.*, vol. 9(2), pp. 13–16.
7. Abdel-Monem A. A., Hurley P. M. 1979, U–Pb dating of zircon from psammitic gneisses, Wadi Abu Rosheid-Wadi Sikait area, Egypt. *Institute of Appl. Geol. Bull. KAUJ, Saudi Arab.*, vol. 2, pp. 165–170.
8. Zaghloul Z. M., Zalata, A. A., Mashaal S. E. 1981, The varietal features and growth trends of zircons in the granitoid rocks of Gabal El-Shayib area, Eastern Desert, Egypt. *Mans. Bull. Sci.*, vol. 8, pp. 405–443.
9. El Gemmizi M. A. 1984, On the occurrence and genesis of mud zircon in the radioactive psammitic gneiss of Wadi Nugrus, Eastern Desert, Egypt. *J. Univ. Kuwait Sci.*, vol. 11, pp. 285–293.
10. Dardier A. M. 1999, Morphology and geochemistry of zircon associated with uranium mineralization in Gattar granitic pluton, north Eastern Desert, Egypt. *J. Min. Soc. Egypt*, vol. 11, pp. 91–104.
11. Hassan I. S. 1997, Mineralogy, petrology and geochemistry of granitoid rocks of St. Katherine area, South Sinai, Egypt. Ph.D. thesis, Eotvos Lorand Univ., Budapest, Hungary, 188 p.
12. Hassan I. S. 2001, Typology and physical changes of zircons from some late Precambrian rocks, southern Sinai, Egypt. Proceeding of the 6th Conference Geology of Sinai for development, Ismailia, pp. 355–369.
13. Belousova E. A.; Griffin W. L., O'Reilly S. Y., Fisher N. J. 2002, Igneous zircon: trace element composition as an indicator of source rock type. *Contrib Mineral Petrol.*, vol. 143, pp. 602–622. https://doi.org/10.1007/s00410-002-0364-7
14. Hoskin P. W. O., Schaltegger U. 2003, The composition of zircon and igneous and metamorphic petrogenesis. *Rev. Miner. Geochem.*, vol. 53,

no. 1, pp. 27–62. https://doi.org/10.2113/0530027
15. El-Mansi M. M., Dardier A. M., Abdel Ghani I. M. 2004, Crystal habit and chemistry of zircon as a guide for uranium redistribution in Gabal Ria El-Garrah area, Eastern Desert, Egypt. *Delta J. Sci*., vol. 28, pp.19–30.
16. Dawoud M. 2004, The nature and origin of U-bearing fluids as revealed from zircon alteration: examples from the Gattarian granites of Egypt. The Sixth International Conference on Geochemistry, Alexandria University, Egypt, 15–16 Sept., pp. 875–891.
17. Abdalla H. A., Helba H., Matsueda H. 2008, Chemistry of Zircon in Rare Metal Granitoids and Associated Rocks, Eastern Desert, Egypt. *Res. Geol*., vol. 59, pp. 51–68. https://doi.org/10.1111/j.1751-3928.2008.00079.x
18. Hoshino M., Kimata M., Nishida N., Shimizu M., Akasaka T. 2010, Crystal chemistry of zircon from granitic rocks, Japan: genetic implications of HREE, U and Th enrichment. *N. Jb. Miner. Abh*., vol. 187(2), pp. 167–188. https://doi.org/10.1127/0077-7757/2010/0177
19. Nardi L. V. S., Formoso M. L. L.; Müller I. F., Fontana E., Jarvis K., Lamarão C. 2013, Zircon/rock partition coefficients of REEs, Y, Th, U, Nb, and Ta in granitic rocks: uses for provenance and mineral exploration purposes. *Chemical Geology*, vol. 335, pp.1–7. https://doi.org/10.1016/j.chemgeo.2012.10.043
20. Breiter K., Lamarão C. N., Borges R. M. K., Dall'Agnol R. 2014, Chemical characteristics of zircon from A-type granites and comparison to zircon of S-type granites. *Lithos*, vol. 192, pp. 208–225. https://doi.org/10.1016/j.lithos.2014.02.004
21. Grimes C. B., Wooden J. L. Cheadle M. J., John B. E. 2015, "Fingerprinting" tectono-magmatic provenance using trace elements in igneous zircon. *Contrib. Mineral. Petrol*., vol. 170(5-6), 46.
22. Omran A. A., Dessouky O. K. 2016, Ra's Abdah of the north Eastern Desert of Egypt: the role of granitic dykes in the formation of radioactive mineralization, evidenced by zircon morphology and chemistry. *Acta Geochimica*, vol. 35(4), pp. 368–380.
23. Abdel-Meguid A. A., Cuney M., Ammar S. E, Ibrahim T. M., Ali K. G., Shahin H. A., Omer S. A., Gaafar I. M., Masoud S. M., Khamis A. A., Haridy M. H., Kamel A. I., Mostafa B. M., Abo Donia A. M., Abdel Gawad A. E., Aly E. M. 2003, Uranium Potential of Eastern Desert Granites, Egypt. Internal Report for Project: EGY/03/014: Technical Assistance by (IAEA), p. 270.
24. Ibrahim M. E., Zalata A. A., Assaf H. S., Ibrahim I. H., Rashed M. A. 2005, El Sella shear zone, South Eastern Desert, Egypt. Example of vein-type uranium deposit. The 9th International Mining, Petroleum and Metallurgical Engineering Conference, pp. 41–55.
25. Ibrahim T. M., Amer T. E., Ali K. G., Omar S. A. 2007, Uranium potentiality and its extraction from El Sela shear zone, south Eastern Desert Egypt. *Fac. Sci. Minufia Univ*. XXI, pp. 1–18.
26. Abd El-Naby H. H., Dawood Y. H. 2008, Natural attenuation of uranium and formation of autunite at the expense of apatite within an oxidizing environment, south Eastern Desert of Egypt. *Appl. Geoch*., vol. 23(12), pp. 3741–3755. https://doi.org/10.1016/j.apgeochem.2008.09.011
27. Ali M. A., Lentz D. R. 2011, Mineralogy, geochemistry and age dating of shear zone-hosted Nb–Ta, Zr–Hf-, Th-, U-bearing granitic rocks in the Ghadir and El-Sella areas, South Eastern Desert, Egypt. *Chin. J. Geoch*., pp. 453–478.
28. Ali K. G. 2013, Structural control of El Sela granites and associated uranium deposits, south Eastern Desert, Egypt. *Arab J. Geosci*., vol. 6(6), pp. 1753–1767.
29. Ramadan T. M., Ibrahim T. M., Said A., Baiumi M. B. 2013, Application of remote sensing in exploration for uranium mineralization in Gabal El Sela area, south Eastern Desert, Egypt. *J. Remote Sens. Space Sci*., vol. 16, 199–210.
30. Abouelnaga H. S. O., El-Shayeb H., Ammar S. E., Haridy H. M. M., Abu Donia A. 2014, Detailed ground radiometric surveys on Gabal El Sela, Southeastern Desert, Egypt. *Arab J. Geosci.*, vol. 7(4), pp. 1577–1586.
31. Gaafar I., Cuney M., Abdel Gawad A. E. 2014, Mineral chemistry of two-mica granite rare metals: impact of geophysics on the distribution of uranium mineralization at El Sela shear zone. *Egypt. Open J. Geol.*, vol. 4, pp. 137–160. https://doi.org/10.4236/ojg.2014.44011
32. Shahin H. A. A. 2014, Zr–Y–Nb–REE mineralization associated with microgranite and basic dykes at EL Sela shear zone, South Eastern Desert, Egypt. *SpringerPlus*, vol. 3, no. 1, 573, pp. 1–12. https://doi.org/10.1186/2193-1801-3-573
33. Abdel Gawad A. E.; Orabi A. H., Bayoumi M. B. 2015, Uranium evaluation and its recovery from microgranite dike at G. El Sela area, South Eastern Desert. *Egypt. Arab J. Geosci.*, pp. 4565–4580. https://doi.org/10.1007/s12517-014-1499-3
34. Abdel Gawad A. E., Ibrahim E. M. 2016, Activity ratios as a technique for studying uranium mobility at El Sela shear zone, southeastern Desert, Egypt. *J. Radioanal Nucl. Chem*., pp. 129–142.
35. Ghoneim M. M., Abdel Gawad A. E. 2018a, Vein-type uranium mineralization in the Eastern Desert of Egypt. *News of the Ural State Mining University*, vol. 1, issue 49, pp. 33–38.
36. Ghoneim M. M., Abdel Gawad A. E. 2018b, Chemical composition of uranium and thorium minerals of El Sela area, Eastern Desert, Egypt. in Russian, pp. 214–216.
37. Abdel Gawad A. E. 2018, Geochemical behaviour of trace and rare earth elements during hydrothermal alteration at El Sela shear zone, Egypt. VIII young geoscientists school, New knowledge about ore-forming processes, 26–30 Nov. 2018, IGEM RAS. Moscow, pp. 439–442.
38. Pupin J. P. 1980, Zircon and granite petrology. *Contrib. Mineral Petrol*., vol. 73(3), pp. 207–220.
39. Vavra G. 1990, On the kinematics of zircon growth and its petrogenetic significance: a cathodoluminescence study. *Contrib. Mineral Petrol*., vol. 106, pp. 90–99.
40. Benisek A., Finger F. 1993, Factors controlling the development of prism faces in granite zircons: a microprobe study. *Contributions to Mineralogy and Petrology*, vol. 114, pp. 441–451.
41. Corfu F., Hanchar J. M., Hoskin P. W. O., Kinny P. 2003, Atlas of zircon textures. *Rev. Miner. Geochem.*, vol. 53, no. 1, pp. 469–500. https://doi.org/10.2113/0530469
42. Pidgeon R. T. 1992, Recrystallisation of oscillatory zoned zircon: some geochronological and petrological implications. *Contributions to Mineralogy and Petrology*, vol. 110, pp. 463–472.
43. Pupin J. P., Turco G. 1972a, Le zircon accessoire en géothermométrie. *Comptes Rendus de l'Académie des Sciences de Paris*, vol. 274(2), pp. 212–214.
44. Pupin J. P., Turco G. 1981, Le zircon, minéral commun significatif des roches endogenes et exogilnes. *Bulletin de Minéralogie*, vol. 104, pp. 724–731.
45. Pupin J. P., Turco G. 1972b, Une typologie originale du zircon accessoire. *Bulletin de la Société Française de Minéralogie*, vol. 95, pp. 348–359.
46. Pupin J. P., Bonin B., Tessier M., Turco G. 1978, Role de l'eau sur les caracteres morphologiques et la cristallisation du zircon dans les granitoides. *Bulletin de la Société Géologique de France*, vol. S7-XX, no. 5, pp. 721–725. https://doi.org/10.2113/gssgfbull.S7-XX.5.721
47. Zhang M., Salje E. K. H., Ewing R. C. 2003, Oxidation state of uranium in metamict and annealed zircon: near-infrared spectroscopic quantitative analysis. *Journal of Physics: Condensed Matter*, vol. 15, no. 20, pp. 3445–3470. http://dx.doi.org/10.1088/0953-8984/15/20/307
48. Geisler-Wierwille T., Pidgeon R. T., Kurtz R., Van Bronswijk W., Schleicher H. 2003, Experimental hydrothermal alteration of partially metamict zircon. *Amer. Min*., vol. 88, pp. 1496–1513. http://dx.doi.org/10.2138/am-2003-1013
49. Martins H. C. B., Abreu J. 2014, The composition of zircon in Variscan granites from Northern Portugal. *Estudios Geológicos*, vol. 70(2), e018. https://doi.org/10.3989/egeol.41729.318.
50. Bao X. 1995, Two Trends of Composition Variation of Zircons and Their Significance in Origin Discrimination. *Acta Min. Sinica*, vol. 15(4), pp. 404–410.
51. Rub M. G., Rub A. K., Salmin U. P. 1994, Compositional features of zircon of rare metal granitoids. *Geochemistry*, vol. 11, pp. 76–91. (*In Russ.*)
52. Larin A. M. 2011, Rapakivi granite and associated rocks. St. Petersburg, 402 p. (*In Russ.*)

The article was received on June 27, 2020

УДК 549.514.81+549.02(620) https://doi.org/10.21440/2307-2091-2020-3-7-18

Морфология и геохимические особенности циркона из интрузивных пород района Эль-Села, Восточная пустыня, Египет

Мохамед Махмуд Фати ГХОНЕЙМ[1, 2*]
Елена Геннадьевна ПАНОВА[1**]
Ахмед Эль-Сайед АБДЕЛ ГАВАД[2***]
Светлана Юрьевна ЯНСОН[1****]

[1]Санкт-Петербургский государственный университет, Санкт-Петербург, Россия
[2]Агентство по атомной энергетике, Каир, Египет

Аннотация

Интрузивные породы в районе Эль-Селы могут быть сложены от самых старых до самых молодых в двухслюдяные гранитные и постгранитные дайки, включающие дайки микрогранитов, долеритов и бостонитов. Циркон - самый распространенный акцессорный минерал. Морфология и геохимические особенности циркона являются хорошими индикаторами эволюции горных пород. Цель работы - определить морфологию, внутреннее строение и химический состав циркона для выявления различий циркона в различных интрузивных породах. Результаты показали, что морфологически циркон в двуслюдяном граните аутоморфный, крупнозернистый с зональностью. Он представлен кристаллами размером до 125 мкм и соответствует S10 и P2. Циркон в постгранитных дайках имеет неправильную форму. Геохимически кристаллы циркона имеют более высокие значения ZrO_2 в ядре, тогда как HfO_2, UO_2, ThO_2 увеличиваются на периферии зональных кристаллов двуслюдяного гранита. Циркон двуслюдяного гранита содержит высокое содержание HfO_2, UO_2, ThO_2 и CaO, но низкое содержание Sc_2O_3. В цирконе микрогранита HfO_2 не обнаружен. TiO_2 в цирконе даек двуслюдяного гранита и бостонита находится за пределами обнаружения. РЗЭ в цирконе изученных интрузивных пород не обнаружены.

Ключевые слова: циркон, морфология, геохимические особенности, интрузивные породы, Эль-Села, Египет.

ЛИТЕРАТУРА

1. Johnson P. R., Woldehaimanot B. 2003, Development of the Arabian-Nubian Shield: perspectives on accretion and deformation in the northern East African Orogen and the assembly of Gondwana. Geological Society London Special Publications, vol. 206, pp. 289–325. http://dx.doi.org/10.1144/GSL.SP.2003.206.01.15
2. Pupin J. P. 1976, Signification des caractères morphologiques du zircon commun des roches en pétrologie: base de la méthode typologique: applications. Thèse de doctorat: Sciences. Université de Nice. Laboratoire de Pétrologie-Minéralogie, Nice, France, 394 p.
3. Read H. H. 1984, Rutley's elements of mineralogy. Delhi, India: Published by S. K. Jam for CBS Publishers and Distributors, 560 p.
4. Deer W. A., Howie R. A., Zussman J. 1992, An introduction to the rock-forming minerals. 2nd edition. London: Longman Scientific & Technical, 696 p. https://doi.org/10.1180/minmag.1992.056.385.20
5. Khaffagy M. B. 1964, The granites of Aswan and their accessory zircons. Unpublished M. Sc. thesis, Assuit University, 192 p.
6. Hussein H. A., Faris M. I., Makram W. 1965, Radioactivity of some accessory minerals especially zircon in some Egyptian granites and pegmatites. *J. Geol.*, vol. 9(2), pp. 13–16.
7. Abdel-Monem A. A., Hurley P. M. 1979, U–Pb dating of zircon from psammitic gneisses, Wadi Abu Rosheid-Wadi Sikait area, Egypt. *Institute of Appl. Geol. Bull. KAUJ, Saudi Arab.*, vol. 2, pp. 165–170.
8. Zaghloul Z. M., Zalata, A. A., Mashaal S. E. 1981, The varietal features and growth trends of zircons in the granitoid rocks of Gabal El-Shayib area, Eastern Desert, Egypt. *Mans. Bull. Sci.*, vol. 8, pp. 405–443.
9. El Gemmizi M. A. 1984, On the occurrence and genesis of mud zircon in the radioactive psammitic gneiss of Wadi Nugrus, Eastern Desert, Egypt. *J. Univ. Kuwait Sci.*, vol. 11, pp. 285–293.
10. Dardier A. M. 1999, Morphology and geochemistry of zircon associated with uranium mineralization in Gattar granitic pluton, north Eastern Desert, Egypt. *J. Min. Soc. Egypt*, vol. 11, pp. 91–104.
11. Hassan I. S. 1997, Mineralogy, petrology and geochemistry of granitoid rocks of St. Katherine area, South Sinai, Egypt. Ph.D. thesis, Eotvos Lorand Univ., Budapest, Hungary, 188 p.
12. Hassan I. S. 2001, Typology and physical changes of zircons from some late Precambrian rocks, southern Sinai, Egypt. Proceeding of the 6th Conference Geology of Sinai for development, Ismailia, pp. 355–369.
13. Belousova E. A.; Griffin W. L., O'Reilly S. Y., Fisher N. J. 2002, Igneous zircon: trace element composition as an indicator of source rock type. *Contrib Mineral Petrol.*, vol. 143, pp. 602–622. https://doi.org/10.1007/s00410-002-0364-7
14. Hoskin P. W. O., Schaltegger U. 2003, The composition of zircon and igneous and metamorphic petrogenesis. *Rev. Miner. Geochem.*, vol. 53, no. 1, pp. 27–62. https://doi.org/10.2113/0530027
15. El-Mansi M. M., Dardier A. M., Abdel Ghani I. M. 2004, Crystal habit and chemistry of zircon as a guide for uranium redistribution in Gabal Ria El-Garrah area, Eastern Desert, Egypt. *Delta J. Sci.*, vol. 28, pp.19–30.
16. Dawoud M. 2004, The nature and origin of U-bearing fluids as revealed from zircon alteration: examples from the Gattarian granites of Egypt. The Sixth International Conference on Geochemistry, Alexandria University, Egypt, 15–16 Sept., pp. 875–891.

✉moh.gho@mail.ru
https://orcid.org/0000-0002-3795-476X
**e.panova@spbu.ru
***ahm.elsay@hotmail.com
****svetlana.janson@spbu.ru

17. Abdalla H. A., Helba H., Matsueda H. 2008, Chemistry of Zircon in Rare Metal Granitoids and Associated Rocks, Eastern Desert, Egypt. *Res. Geol*., vol. 59, pp. 51–68. https://doi.org/10.1111/j.1751-3928.2008.00079.x
18. Hoshino M., Kimata M., Nishida N., Shimizu M., Akasaka T. 2010, Crystal chemistry of zircon from granitic rocks, Japan: genetic implications of HREE, U and Th enrichment. *N. Jb. Miner. Abh*., vol. 187(2), pp. 167–188. https://doi.org/10.1127/0077-7757/2010/0177
19. Nardi L. V. S., Formoso M. L. L.; Müller I. F., Fontana E., Jarvis K., Lamarão C. 2013, Zircon/rock partition coefficients of REEs, Y, Th, U, Nb, and Ta in granitic rocks: uses for provenance and mineral exploration purposes. *Chemical Geology*, vol. 335, pp.1–7. https://doi.org/10.1016/j.chemgeo.2012.10.043
20. Breiter K., Lamarão C. N., Borges R. M. K., Dall'Agnol R. 2014, Chemical characteristics of zircon from A-type granites and comparison to zircon of S-type granites. *Lithos*, vol. 192, pp. 208–225. https://doi.org/10.1016/j.lithos.2014.02.004
21. Grimes C. B., Wooden J. L. Cheadle M. J., John B. E. 2015, "Fingerprinting" tectono-magmatic provenance using trace elements in igneous zircon. *Contrib. Mineral. Petrol*., vol. 170(5-6), 46.
22. Omran A. A., Dessouky O. K. 2016, Ra's Abdah of the north Eastern Desert of Egypt: the role of granitic dykes in the formation of radioactive mineralization, evidenced by zircon morphology and chemistry. *Acta Geochimica*, vol. 35(4), pp. 368–380.
23. Abdel-Meguid A. A., Cuney M., Ammar S. E, Ibrahim T. M., Ali K. G., Shahin H. A., Omer S. A., Gaafar I. M., Masoud S. M., Khamis A. A., Haridy M. H., Kamel A. I., Mostafa B. M., Abo Donia A. M., Abdel Gawad A. E., Aly E. M. 2003, Uranium Potential of Eastern Desert Granites, Egypt. Internal Report for Project: EGY/03/014: Technical Assistance by (IAEA), p. 270.
24. Ibrahim M. E., Zalata A. A., Assaf H. S., Ibrahim I. H., Rashed M. A. 2005, El Sella shear zone, South Eastern Desert, Egypt. Example of vein-type uranium deposit. The 9th International Mining, Petroleum and Metallurgical Engineering Conference, pp. 41–55.
25. Ibrahim T. M., Amer T. E., Ali K. G., Omar S. A. 2007, Uranium potentiality and its extraction from El Sela shear zone, south Eastern Desert Egypt. *Fac. Sci. Minufia Univ*. XXI, pp. 1–18.
26. Abd El-Naby H. H., Dawood Y. H. 2008, Natural attenuation of uranium and formation of autunite at the expense of apatite within an oxidizing environment, south Eastern Desert of Egypt. *Appl. Geoch*., vol. 23(12), pp. 3741–3755. https://doi.org/10.1016/j.apgeochem.2008.09.011
27. Ali M. A., Lentz D. R. 2011, Mineralogy, geochemistry and age dating of shear zone-hosted Nb–Ta, Zr–Hf-, Th-, U-bearing granitic rocks in the Ghadir and El-Sella areas, South Eastern Desert, Egypt. *Chin. J. Geoch*., pp. 453–478.
28. Ali K. G. 2013, Structural control of El Sela granites and associated uranium deposits, south Eastern Desert, Egypt. *Arab J. Geosci*., vol. 6(6), pp. 1753–1767.
29. Ramadan T. M., Ibrahim T. M., Said A., Baiumi M. B. 2013, Application of remote sensing in exploration for uranium mineralization in Gabal El Sela area, south Eastern Desert, Egypt. *J. Remote Sens. Space Sci.*, vol. 16, 199–210.
30. Abouelnaga H. S. O., El-Shayeb H., Ammar S. E., Haridy H. M. M., Abu Donia A. 2014, Detailed ground radiometric surveys on Gabal El Sela, Southeastern Desert, Egypt. *Arab J. Geosci.*, vol. 7(4), pp. 1577–1586.
31. Gaafar I., Cuney M., Abdel Gawad A. E. 2014, Mineral chemistry of two-mica granite rare metals: impact of geophysics on the distribution of uranium mineralization at El Sela shear zone. *Egypt. Open J. Geol.*, vol. 4, pp. 137–160. https://doi.org/10.4236/ojg.2014.44011
32. Shahin H. A. A. 2014, Zr–Y–Nb–REE mineralization associated with microgranite and basic dykes at EL Sela shear zone, South Eastern Desert, Egypt. *SpringerPlus*, vol. 3, no. 1, 573, pp. 1–12. https://doi.org/10.1186/2193-1801-3-573
33. Abdel Gawad A. E.; Orabi A. H., Bayoumi M. B. 2015, Uranium evaluation and its recovery from microgranite dike at G. El Sela area, South Eastern Desert. *Egypt. Arab J. Geosci.*, pp. 4565–4580. https://doi.org/10.1007/s12517-014-1499-3
34. Abdel Gawad A. E., Ibrahim E. M. 2016, Activity ratios as a technique for studying uranium mobility at El Sela shear zone, southeastern Desert, Egypt. *J. Radioanal Nucl. Chem*., pp. 129–142.
35. Ghoneim M. M., Abdel Gawad A. E. 2018a, Vein-type uranium mineralization in the Eastern Desert of Egypt. *News of the Ural State Mining University*, vol. 1, issue 49, pp. 33–38.
36. Ghoneim M. M., Abdel Gawad A. E. 2018b, Chemical composition of uranium and thorium minerals of El Sela area, Eastern Desert, Egypt. VII Readings in memory of S.N.Ivanov, in Russian, pp. 214–216.
37. Abdel Gawad A. E. 2018, Geochemical behaviour of trace and rare earth elements during hydrothermal alteration at El Sela shear zone, Egypt. VIII young geoscientists school, New knowledge about ore-forming processes, 26–30 Nov. 2018, IGEM RAS. Moscow, pp. 439–442.
38. Pupin J. P. 1980, Zircon and granite petrology. *Contrib. Mineral Petrol*., vol. 73(3), pp. 207–220.
39. Vavra G. 1990, On the kinematics of zircon growth and its petrogenetic significance: a cathodoluminescence study. *Contrib. Mineral Petrol*., vol. 106, pp. 90–99.
40. Benisek A., Finger F. 1993, Factors controlling the development of prism faces in granite zircons: a microprobe study. *Contributions to Mineralogy and Petrology*, vol. 114, pp. 441–451.
41. Corfu F., Hanchar J. M., Hoskin P. W. O., Kinny P. 2003, Atlas of zircon textures. *Rev. Miner. Geochem.*, vol. 53, no. 1, pp. 469–500. https://doi.org/10.2113/0530469
42. Pidgeon R. T. 1992, Recrystallisation of oscillatory zoned zircon: some geochronological and petrological implications. *Contributions to Mineralogy and Petrology*, vol. 110, pp. 463–472.
43. Pupin J. P., Turco G. 1972a, Le zircon accessoire en géothermométrie. *Comptes Rendus de l'Académie des Sciences de Paris*, vol. 274(2), pp. 212–214.
44. Pupin J. P., Turco G. 1981, Le zircon, minéral commun significatif des roches endogenes et exogilnes. *Bulletin de Minéralogie*, vol. 104, pp. 724–731.
45. Pupin J. P., Turco G. 1972b, Une typologie originale du zircon accessoire. *Bulletin de la Société Française de Minéralogie*, vol. 95, pp. 348–359.
46. Pupin J. P., Bonin B., Tessier M., Turco G. 1978, Role de l'eau sur les caracteres morphologiques et la cristallisation du zircon dans les granitoides. *Bulletin de la Société Géologique de France*, vol. S7-XX, no. 5, pp. 721–725. https://doi.org/10.2113/gssgfbull.S7-XX.5.721
47. Zhang M., Salje E. K. H., Ewing R. C. 2003, Oxidation state of uranium in metamict and annealed zircon: near-infrared spectroscopic quantitative analysis. *Journal of Physics: Condensed Matter*, vol. 15, no. 20, pp. 3445–3470. http://dx.doi.org/10.1088/0953-8984/15/20/307
48. Geisler-Wierwille T., Pidgeon R. T., Kurtz R., Van Bronswijk W., Schleicher H. 2003, Experimental hydrothermal alteration of partially metamict zircon. *Amer. Min*., vol. 88, pp. 1496–1513. http://dx.doi.org/10.2138/am-2003-1013
49. Martins H. C. B., Abreu J. 2014, The composition of zircon in Variscan granites from Northern Portugal. *Estudios Geológicos*, vol. 70(2), e018. https://doi.org/10.3989/egeol.41729.318.
50. Bao X. 1995, Two Trends of Composition Variation of Zircons and Their Significance in Origin Discrimination. *Acta Min. Sinica*, vol. 15(4), pp. 404–410.
51. Rub M. G., Rub A. K., Salmin U. P. 1994, Compositional features of zircon of rare metal granitoids. *Geochemistry*, vol. 11, pp. 76–91. (*In Russ.*)
52. Ларин А.М. Граниты рапакиви и ассоциирующие породы. СПб.: Наука, 2011. 402 с.

Статья поступила в редакцию 27 июня 2020 года